

Palaeomagnetism of Late Cretaceous-Paleocene igneous rocks from the western part of the Antarctic Peninsula (Argentine Islands Archipelago)

Vladimir BAKHMUTOV and Victor SHPYRA



Bakmutov V. and Shpyra V. (2011) – Palaeomagnetism of Late Cretaceous-Paleocene igneous rocks from the western part of Antarctic Peninsula (Argentine Islands Archipelago). *Geol. Quart.*, 55 (4): 285–300. Warszawa.

A collection of 360 oriented samples of igneous rocks from the western part of the Antarctic Peninsula (Argentine Islands Archipelago, Penola Strait area), has yielded well-defined palaeomagnetic directions. Age determinations by various methods showed a Late Cretaceous-Paleocene time interval for the rocks studied. The characteristic remanent magnetisation (ChRM) was isolated by a stepwise thermal demagnetisation mostly in the temperature interval 450–580°C. It is evidently a primary magnetisation. The rocks along the coastline of the western part of the Antarctic Peninsula (AP) were emplaced during the Cretaceous Normal Superchron while the rocks from the islands with reversed polarity are of Paleocene. New Cretaceous (112–85 Ma) and Paleocene (60 Ma) palaeomagnetic poles for the passive continental margin of the Antarctic Peninsula fit well with a synthetic East Antarctica apparent polar wander path and confirms that the AP did not undergo latitudinal displacement for the last 100 Ma. The palaeomagnetic pole for 60 Ma shows a slight shift from palaeopoles obtained for the South Shetland Islands which implies that the South Shetland block is characterized by own tectonic evolution and probable anticlockwise rotation during the Paleocene.

Vladimir Bakmutov and Victor Shpyra, Institute of Geophysics, National Academy of Science of the Ukraine, Palladin av. 32, 03680 Kiev-142, Ukraine, e-mail: bakhm@igph.kiev.ua (received: July 25, 2011; accepted: November 20, 2011).

Key words: Cretaceous, Paleocene, Antarctic Peninsula, palaeomagnetism.

INTRODUCTION

In contrast to East Antarctica, which consists mainly of Precambrian rocks, West Antarctica is built out of Phanerozoic complexes (Grikurov, 1973; Dalziel and Elliot, 1982) comprising a series of mobile belts which include at least four major crustal blocks (the Antarctic Peninsula, Thurston Island, the Ellsworth–Whitmore Mountains and Marie Byrd Land) with independent Mesozoic and Cenozoic tectonic histories. During the break-up of Gondwana these blocks moved relative to each other and to the East Antarctic Craton (Dalziel and Elliot, 1982; Dalziel and Lawver, 2001).

The tectonic history of the Antarctic Peninsula (AP), the largest crustal block of West Antarctica, relates to Gondwana break-up and tectonic processes that occurred along the southeast Pacific continental margin. Recent geophysical and geological studies suggest that the AP is a composite magmatic arc which is considered to be formed of three domains that amalgamated during the mid-Cretaceous (Vaughan and Storey, 2000; Vaughan *et al.*, 2002; Ferraccioli *et al.*, 2006). In the Late Cretaceous the AP was affected by southeastwards

subduction of Phoenix Plate, all of which was subducted at the Western AP continental margin (Larter *et al.*, 2002). Through the late Mesozoic and Cenozoic, subduction has stopped progressively from south-west to north-east as a result of a series of ridge-trench collisions (Larter and Barker, 1991). Subduction is only active today in the northern part of the AP adjacent to the South Shetland Islands located between the Shackleton and Hero fracture zones.

In a plate tectonic reconstruction where South America is fixed, the AP underwent a relative southwards latitudinal motion from the break-up of Gondwana until about 118 Ma (Ghidella *et al.*, 2002). Since 90 Ma the AP block went through clockwise rotation to its current position (Cunningham *et al.*, 1995; Ghidella *et al.*, 2002). The final separation between the AP and Patagonia occurred around 40 Ma when the Scotia Plate was formed (Barker, 2001).

Most palaeogeographic reconstructions for the AP and South America are based on sea-floor magnetic anomalies. However, palaeomagnetic studies have also been carried out to provide constraints on the relative positions of South America, the Antarctic Peninsula and East Antarctica. For example, according to Grunow (1993), the Antarctic Peninsula underwent

a clockwise rotation from 175 to 155 Ma (which was related to the opening of the Weddell Sea), and a counterclockwise rotation between 155 and 130 Ma.

Palaeomagnetic results for the Antarctic Peninsula have already been reported in a number of studies (Blundell, 1962; Dalziel *et al.*, 1973; Kellogg and Reynolds, 1978; Valencio *et al.*, 1979; Kellogg, 1980; Longshaw and Griffiths, 1983; Watts *et al.*, 1984; Grunow, 1993; Parés and Dinarès-Turell, 1999; Nawrocki *et al.*, 2010; Poblete *et al.*, 2011). Some of these constrain the relative motion of the Antarctic Peninsula since the mid-Cretaceous and allow the quantification of tectonic rotation between the different blocks recognized within the area. In recent work (Poblete *et al.*, 2011) the authors note remagnetisation of the Paleozoic and Jurassic rocks in the area which could reflect an important tectonic event during Cretaceous time in the northern Antarctic Peninsula and its association with the well-documented mid-Cretaceous Palmer Land Event (Vaughan *et al.*, 2002).

The previously published Cretaceous and Cenozoic palaeomagnetic results as well as those published here come mainly from volcanic and intrusive rocks. The magnetisation of these rocks is mainly primary and palaeomagnetic data could be confidently used for the apparent polar wander path (APWP) determination for the Antarctic Peninsula with subsequent palaeotectonic reconstructions. However, only a few studies (Watts *et al.*, 1984; Grunow, 1993; Nawrocki *et al.*, 2010; Poblete *et al.*, 2011) provided detailed palaeomagnetic and geological information. These papers presented the palaeomagnetic results of three areas: the South Shetland Islands, the northern part of Graham Land and Gerlache Strait (the last one includes the Penola Strait area). These are different parts of the continental margin of the AP which are characterized by distinct deep structure and tectonic evolution (Yegorova *et al.*, 2011). The active margin segment of the northern AP is characterized by ongoing subduction beneath the South Shetland Trench and active continental rifting in the Bransfield Strait. The South Shetland Islands represent the exposed part of a huge crustal diapir, which is composed mostly of Cretaceous ultramafic rocks. The passive segment, which was superimposed along a palaeosubduction zone within the AP margin near Anvers Island, is located to the south and has the typical crustal structure of a passive continental margin.

In this paper we present new palaeomagnetic data from the Late Cretaceous and Paleocene rocks collected in the western part of the AP (Penola Strait area). This region is characterized by termination of tectonic activity in the Late Miocene–Early Pliocene and belongs to the passive continental margin. Some of the mean poles previously published for this area correspond to a low number of sites. Our new data, which are broadly consistent with previous results from this area (Blundell, 1962; Grunow, 1993), may be used to better constrain the tectonic model of this key region of Antarctica.

GEOLOGY AND RADIOMETRIC DATING

About 80% of rocks exposed on the islands of the AP shelf as well as on the mainland are formed by plutonic rocks of the

AP batholith (Leat *et al.*, 1995) and volcanic rocks of the AP Volcanic Group (Thompson and Pankhurst, 1983). The plutonic rocks were emplaced within the period ~240 to 10 Ma with an Early Cretaceous peak of activity (Leat *et al.*, 1995). The Early Cretaceous plutonic rocks of gabbro-granite composition (with a prevalence of diorites) constitute widespread plutons and batholiths (Leat *et al.*, 1995; Willan and Kelley, 1999). The acid rocks are younger than the basic ones (Rex, 1976). The volcanic rocks of the AP Volcanic Group occur as veins, dykes and represented by andesites, diabases, basalts, rhyolites, dolerites and dacites (Weaver *et al.*, 1982; Riley *et al.*, 2001).

As mentioned above, the AP is a composite magmatic arc terrane formed at the Pacific margin of Gondwana. At present most of the continental margin of the AP is passive, but the imprints of former tectonic events are recorded in geophysical fields (gravity and magnetic anomalies). We investigated the region located south of Anvers Island, i.e. the passive continental margin of the northern part of the AP, which is characterized by a juxtaposition of two crustal blocks of different structure and, probably, affinities, which collided during the Late Jurassic. These domains represent (in the east) the crustal domain of Pacific margin of Gondwana and a block of accretional tectonics between the latter and the oceanic domain of the Bellingshausen Sea.

The geological setting of Penola Strait area and locations of palaeomagnetic sites are shown in Figure 1. The petrology of this region and of the adjacent offshore islands is described in Hooper (1962), Elliot (1964) and Curtis (1966). The volcanic rocks of the AP Volcanic Group comprising andesite lavas and pyroclastic rocks compose mainly the West Antarctic Peninsula coast while the plutonic rocks of an initial gabbro intrusion phase of the Andean Intrusive Suite are exposed both along the coast line and on the western islands (Fig. 1).

The radiometric ages used below are based on a compilation of previously published data (Rex, 1976; Fleming and Thomson, 1979; Pankhurst, 1982, 1983; Leat *et al.*, 1995; Tangeman *et al.*, 1996) and on recent U-Pb zircon results for the rocks studied in this work (Gładkochub *et al.*, 2009; Gładkochub, pers. comm.). A summary of age determinations as reported in the original references are given in Table 1.

WESTERN COAST OF THE ANTARCTIC PENINSULA

Banded hornblende gabbros crop out on the NW point of Cape Tuxen (Curtis, 1966). Granodiorite dykes intruding the gabbros are observed in cliff faces. Zircon U-Pb dating of quartz-diorite from the prominent point of Cape Tuxen yields an age of 85.2 ± 0.7 Ma (Tangeman *et al.*, 1996; Table 1). U-Pb dating of quartz-diorite from the base of Mount Demaria and from granodiorite collected approximately 1 km south-east of Cape Tuxen yielded ages 84.8 ± 0.5 Ma and 84.5 ± 0.9 Ma respectively (Tangeman *et al.*, 1996). Recent U-Pb dating of zircon crystallisation in the gabbros from Cape Tuxen yielded an age of 88.1 ± 1.1 (Gładkochub *et al.*, 2009). An $^{39}\text{Ar}/^{40}\text{Ar}$ plateau age provides the age of the closure of the Ar-Ar isotopic system of plagioclase (150°C) in the gabbro as 70.9 ± 1.1 Ma. It this could mean that the cooling of this intrusion to 150°C took about 17 million years.

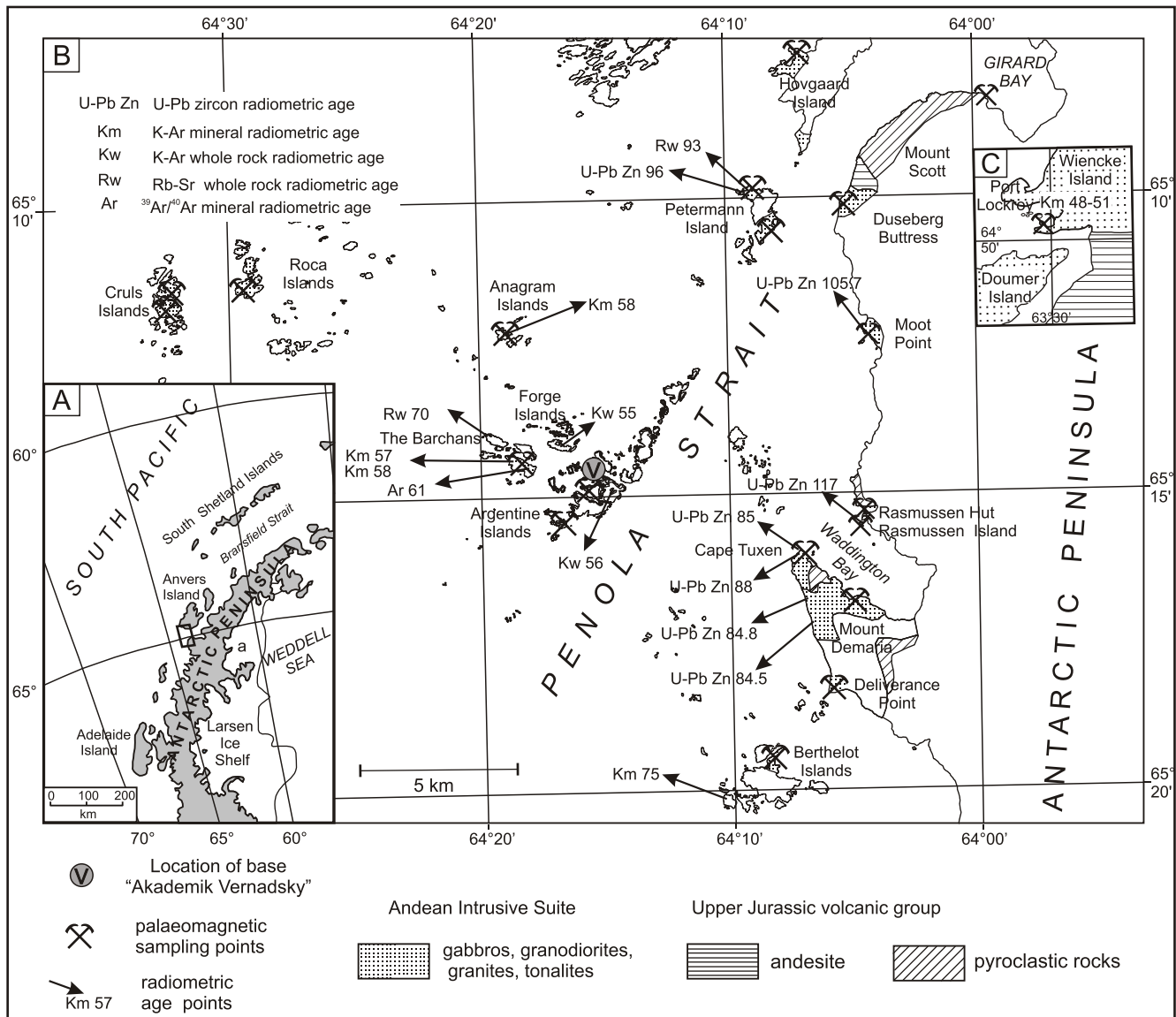


Fig. 1. Location of rock samples in the Argentine Island Archipelago area

A – map of the Antarctic Peninsula, the small rectangle in the centre of the map depicts the location of the region investigated, details of the site locations are shown in B and C; B – Penola Strait area (Argentine Islands Archipelago) and the western coast of the Antarctic Peninsula; C – Wiencke Island, near Port Lockroy; geological setting modified from Curtis (1966)

Moot Point forms a series of low islands and a promontory along Penola Strait and consists of medium-grained, biotite + hornblende bearing diorite cut by nearly vertical north-south trending mafic dykes. U-Pb dating of quartz-diorite yields an age of 105.7 ± 0.7 Ma (Tangeman *et al.*, 1996). There are no age determinations from the mafic dykes, but they yield palaeomagnetic directions indistinguishable from the diorite (Grunow, 1993) and were not observed cutting the Cape Tuxen rocks which suggests that the dykes are older than ~85 Ma and likely comagmatic with the diorite.

The outcrops on the promontory of the headland near Rasmussen Hut and on Rasmussen Island, located over hundred metres from the AP south of Rasmussen Hut, are composed of different gabbros, diabase, granodiorite and granite, cut by comagmatic mafic dykes. The coarse-grained pink granite on

Rasmussen Island yielded U-Pb zircon age of 117.0 ± 0.8 Ma (Tangeman *et al.*, 1996), which differs markedly from Rb-Sr data (128 ± 3 Ma) obtained at this place by Pankhurst (1982).

Four kilometres north of Moot Point opposite the Petermann and Hovgaard Islands the most spectacular exposures of volcanic rocks of the AP Volcanic Group are located on the mainland coast of Penola Strait and on the shores bordering Lemaire Channel. The volcanic rocks crop out along the coast of a distance of about 1.5 km and had been folded into an asymmetrical syncline with its axis trending NW to SE. They have been intruded by diorite about 0.8 km north of Duseberg Buttress. The sampling in this region was carried out at three points: diorites of Duseberg Buttress, basalts at the bottom of Scott Mount and gabbro in the SW of Girard Bay. No ages are known for these points, but analysis of the geological structures

Table 1

Results of the age-dating of AP batholith plutonic rocks which were studied palaeomagnetically

Locality	Lat., Long.	Rock types	Radiometric method	Mineral analysed	Analyses reference number (by Reference)	Age [Ma]	Reference
Cape Tuxen and Deliverance Point	64°07'W 65°16'S	quartz-diorite	U-Pb	zircon	AP90-11H	85.2 ±0.7	Tangeman <i>et al.</i> (1996)
	64°071'W 65°161'S	gabbro	U-Pb	zircon		88.1 ±1.1	Gladkochub <i>et al.</i> (2009)
	64°066'W 65°171'S	quartz-diorite	U-Pb	zircon	AP90-11J	84.8 ±0.5	Tangeman <i>et al.</i> (1996)
	64°06'W 65°18'S	granodiorite	U-Pb	zircon	AP90-11K	84.5 ±0.9	Tangeman <i>et al.</i> (1996)
Moot Point	64°045'W 65°123'S	quartz-diorite	U-Pb	zircon	AP90-11A	105.7 ±0.7	Tangeman <i>et al.</i> (1996)
Rasmussen Island	64°045'W 65°155'S	granite	U-Pb	zircon	AP90-11F	117.0 ±0.8	Tangeman <i>et al.</i> (1996)
		pink granite	Rb-Sr			128 ±3	Pankhurst (1982)
Petermann Island	64°09'W 65°10'S	diorite/granite	Rb-Sr whole rock			93 ±8	Pankhurst (1982)
		quartz-diorite	U-Pb	zircon		95.9 ±1 96.1 ±0.7	Gladkochub (pers. comm.)
Berthelot Islands	64°10'W 65°19'S	diorite	K-Ar	pyroxene	IDB597	73 ±6	Rex (1976)
Argentine Islands Archipelago	64°15'W 65°15'S	diorite/ granodiorite/ aplite	Rb-Sr			55 ±3	Pankhurst (1982)
Forge Islands	64°18'W 65°14'S	hornblendite	K-Ar	hornblende	IDB801	54 ±2	Rex (1976)
Anagram Islands	64.192'W 65.123'S		K-Ar			58	Fleming and Thomson (1979)
The Barchans, South Island	64°20'W 65°14'S	quartz-diorite	K-Ar	biotite	IDB574 IDB701 IDB583	56 ±2 56 ±2 57 ±2	Rex (1976)
The Barchans, South Island	64°18'W 65°145'S	granodiorite	³⁹ Ar/ ⁴⁰ Ar	biotite		60.9 ±0.1	Gladkochub <i>et al.</i> (2009)
The Barchans, Western Island		granodiorite	Rb-Sr whole rock			70	Fleming and Thomson (1979)
Goudier Island, Port Lockroy	63°31'W 64°50'S	quartz-diorite	K-Ar	biotite hornblende	IDB514 IDB539	51 ±2 51 ±2	Rex (1976)
Port Lockroy	63°30'W 64°49'S	quartz-diorite	K-Ar	biotite	IDB687	48 ±2	Rex (1976)
				hornblende	IDB711	51 ±2	
				biotite	IDB603	49 ±2	

indicates similarity between diorites from Duseberg Buttress and diorites from Moot Point, as well as between gabbros on Girard Bay and gabbros on Petermann Island and Cape Tuxen. Based on this similarity we assume that the ages of the rocks of these sites correspond to the Late Cretaceous.

NEIGHBOURING ISLANDS

Gabbros and quartz-diorites crop out in the NNW part of the Petermann Island while the central part is formed of granodiorites. In the NW part of Petermann Island, hornblende-gabbros have been intruded by granodiorite. Results of Rb-Sr whole rock radiometric dating reported by Pankhurst (1982) yielded an age of 93 ±8 Ma. U-Pb dating of zircon from quartz-diorite gave an age of 96 Ma (Gladkochub, pers. comm.).

The gabbros and diorites make up the northern part of the Berthelot Islands. Visually the gabbros are similar to the rocks

of the outcrop on the Cape Tuxen. The K-Ar data obtained for diorite from the southern part of the islands yield an age of 73 ±6 Ma (Rex, 1976).

A number of islands located across an area of 6 × 6 km have a common geographic name: the Argentine Islands (Fig. 1). The two biggest (Galindez and Winter) islands are well-known as the Ukrainian Antarctic station "Akademik Vernadsky" (the former British base "Faraday") and an old British base, respectively, are located there. The archipelago is separated from the mainland by the deep Penola Strait, which geologically is a fault between the Antarctic Peninsula and western islands. The western part of the archipelago the Argentine Islands and other western archipelagoes are composed of plutonic rocks which outcrop on the Barchans Islands, Forge Islands, Anagram Islands and in the area further to the west. The eastern part of the archipelago is composed mainly of AP Volcanic Group rocks (andesite lavas and associated pyroclastic rocks, which have been metamorphosed and metasomatized) and separated from

the western plutonic rocks by a sublongitudinal contact zone about 1000 m wide. The object of our research on the Argentine Islands Archipelago was only plutonic rocks. Gabbros, norites and tonalites occur mainly on the Anagram Islands and granodiorites crop out principally in the Barchans and the Forge Islands. K-Ar and Rb-Sr data indicate that the age of these rocks is Paleocene (55–70 Ma; Table 1). Dating of the quartz-diorite from the south island of the Barchans Islands by K-Ar mineral radiometric ages (biotite) yielded 56–57 Ma (Rex, 1976). The K-Ar age of the hornblende from Forge Islands is 54 ± 2 Ma (Rex, 1976) and Rb-Sr dating of the North Barchans Island rocks yielded an age of 70 Ma (Fleming and Thomson, 1979). The K-Ar mineral radiometric age from the Anagram Islands is 58 Ma (Fleming and Thomson, 1979), and the Rb-Sr age is 55 ± 3 Ma. Recent $^{39}\text{Ar}/^{40}\text{Ar}$ dating of biotite from quartz-diorite of the South Barchans Island yielded an age of 60.9 ± 0.1 Ma (Gladkochub *et al.*, 2009).

Diorites, quartz-diorites and granodiorites were sampled in the western part of Wiencke Island located 50 km to the NE of the Argentine Islands (Fig. 1C). The K-Ar radiometric ages from quartz-diorite (biotite and hornblende) from Goudier Island, Port Lockroy, fall in the time interval 48–51 Ma (Rex, 1976; Table 1).

PALAEOMAGNETIC METHODOLOGY

A representative collection of rocks was sampled during several Ukrainian Antarctic season expeditions. About 360 oriented samples were drilled or collected as hand samples both on the western coast of the AP and on the adjoining islands. The sampling of each site covered the maximum accessible (ice-free) area. All samples were collected from blocky, solid and relatively unaltered intrusions and partially from comagmatic dykes thus maximizing the suitability of rocks for palaeomagnetic experiments.

The natural remanent magnetisation (NRM) of samples is typically less than 1 A/m, which is too small to affect the orientation with a magnetic compass. A correction to the field mea-

surements has been made to offset the local magnetic declination of 16°E .

The palaeomagnetic measurements were carried out in the laboratory of the Institute of Geophysics of the National Academy of Sciences of Ukraine in Kiev. The samples were cut into standard cylinders or into cubes 20 mm in length. The specimens were stored in a magnetically shielded room. The vectors of characteristic remanent magnetisation (ChRM) were isolated by both stepwise thermal and alternating field (AF) demagnetisation. Stepwise thermal demagnetisation of up to $600\text{--}610^\circ\text{C}$ in 15–20 steps was carried out using a *MMTD80* oven. After each heating step the susceptibility at room temperature was measured to monitor possible mineralogical changes. A *JR-6* spinner magnetometer and *MFK1* kappabridge were used for magnetisation and susceptibility measurements, respectively. The hysteresis loop parameters were measured by a VSM magnetometer of the Institute of Geophysics, Polish Academy of Sciences. Some duplicate specimens were subjected to AF demagnetisation using a *LDA-3A* demagnetizer, and these results were consistent with the thermal demagnetisation data. During AF demagnetisation about 70–90% of the initial intensity of NRM was removed in a field of less than 50 mT, which is characteristic of low-medium coercivities of magnetic carriers, likely magnetite or titanomagnetite.

The magnetic mineralogy experiments and magnetic properties of samples are described in Shcherbakova *et al.* (2009). Thermomagnetic curves $I_s(T)$ exhibit good thermal stability of those ferrimagnetic minerals with Curie temperatures of $570\text{--}590^\circ\text{C}$ (Fig. 2A). These data indicate that the mineral is magnetite or (and) Ti-poor magnetite. Most of the samples demonstrate a good similarity between the NRM(T) and TRM(T) thermomagnetic curves over a wide temperature range (Fig. 2B) which confirms the thermal stability of the ferromagnetic minerals within the samples and strengthens the argument that the NRMs are TRMs.

In order to assess the magnetic hardness and mineralogy of the samples, hysteresis loop parameters, such as coercive force H_c , remanent coercive force H_{cr} , saturation magnetisation I_s and remanent saturation magnetisation, I_{rs} were analysed. The ratios I_{rs}/I_s and H_{cr}/H_c are plotted on a Day plot (Day *et al.*, 1977)

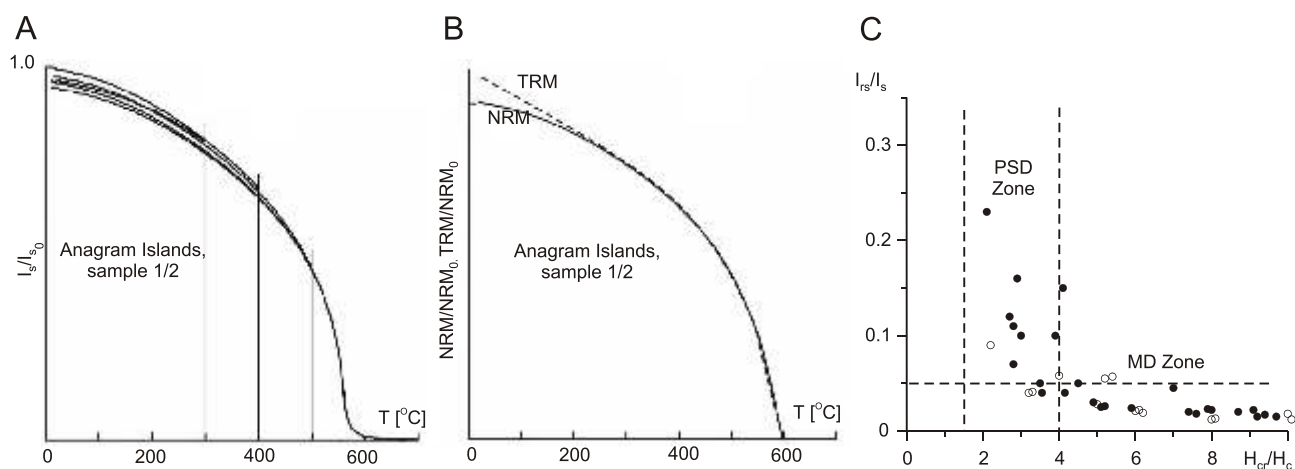


Fig. 2A – thermomagnetisation curve $I_s(T)/I_{s_0}(T)$; B – continuous thermal demagnetisation curves of NRM(T) (solid line), TRM(T) acquired in $H_{lab} = 20 \mu\text{T}$ (dashed line) for representative sample: the curves are normalized to the corresponding NRM value (Shcherbakova *et al.*, 2009); C – day plots for samples from the western coast of the AP (solid circles) and neighbouring islands (open circles)

and fall in either the MD or PSD band: $I_r/I_s = 0.015\text{--}0.23$, $H_{cr}/H_c = 2\text{--}10$, which suggests the presence of both relatively fine and coarse magnetic grains (Fig. 2C).

The microscopic analysis confirmed the presence of magnetite as the main magnetic carrier and revealed the existence of a large ferromagnetic grain together with relatively small magnetite grains dispersed in the silicate matrix (Shcherbakova *et al.*, 2009). Results of energy dispersive X-ray (EDX) analysis carried out for these grains showed the presence of near-magnetite/near-ilmenite intergrowths together with the presence of near-magnetite PSD size grains. This is additional evidence that the NRM of such the grains is primary, is of thermoremanent origin and that the carriers of NRM are predominantly SD-PSD grains. The most likely explanation of both thermomagnetic and electron-microscopic observations are that the main carriers of TRM belong to the small SD-PSD fraction whereas the grains responsible for the hysteresis properties (I_r/I_s and H_{cr}/H_c ratios) reflect the presence of coarse grains (Shcherbakova *et al.*, 2009).

Results of magnetic measurements were processed with the *Remasoft 3.0* program (Chadima and Hrouda, 2006). The ChRM vector of each specimen was determined using the least-squares method (Kirschvink, 1980). The palaeodirections of isolated components obtained were considered as meaningful if they have been defined by three or more collinear demagnetisation steps with a maximum angular deviation of less than 5° . The high stability linear segments were converging toward the origin.

PALAEOMAGNETIC RESULTS

WESTERN COAST OF ANTARCTIC PENINSULA

Cape Tuxen and Deliverance Point. Early palaeomagnetic studies of these rocks determined the NRM directions as $D = 9^\circ$, $I = -77^\circ$ (mean of 8 samples from Cape Tuxen area; Blundell, 1962) and as $D = 4.7^\circ$, $I = -75.2^\circ$ (mean of three sites of granodiorite and three sites of gabbros; Grunow, 1993).

Along the coastline of the AP we collected gabbros on the NW prominent point of Cape Tuxen, granodiorites on the south coast of Waddington Bay (three kilometres to south-east from Cape Tuxen) and granodiorites of Deliverance Point (three kilometres to the south along the sea coast). Palaeomagnetic study of these rocks revealed mainly a single N-polarity component of NRM both in gabbro and granodiorite samples, and some samples are characterized by a second component of between $100\text{--}350^\circ\text{C}$ (Fig. 3A). The Cape Tuxen site direction ($D = 2.8^\circ$, $I = -79.1^\circ$) is in agreement with the data reported by Blundell (1962) and Grunow (1993). The other two sites have similar inclinations, but a small deviation of declinations (the Waddington Bay granodiorite is $D = 13.2^\circ$, $I = -76.4^\circ$; granodiorites from Deliverance Point yield $D = 28.5^\circ$, $I = -77.5^\circ$; Table 2).

Moot Point. Previous research by (Grunow, 1993) suggest two distinct components of NRM from the diorites. The mean direction of the A-component, obtained from five sites, had $D = 23.8^\circ$ and $I = -71.2^\circ$. In some diorite samples, a second,

B-component of NRM, was isolated (13 samples, $D = 297.2^\circ$, $I = -76.3^\circ$).

Our sampling was made on the coast area of the promontory of the AP (diorite) and on the western part of the biggest unnamed island located several hundred metres opposite to the promontory (granodiorite and subvertical mafic dyke in central part of island). In our experiments the demagnetisation curves were similar to the data from Cape Tuxen area and only one N-polarity component of NRM in diorite and granodiorite samples ($D = 12.6^\circ$, $I = -69.6^\circ$ and $D = 39.0^\circ$, $I = -63.8^\circ$, respectively) has been revealed (Table 2). The mean direction of the diorite is close to the A-component obtained by Grunow (1993), but granodiorite samples are characterized by scattering $\alpha_{95} = 14.3$ and display about a 26° difference in declination relative to diorites from the mainland. Two samples from the mafic dyke also show the N-polarity component but they were not included in the statistics.

Rasmussen Hut and Rasmussen Island. Stepwise thermal demagnetisation performed on these rocks by Grunow (1993), indicated a single component NRM for both the granite and mafic dykes from Rasmussen Island with a mean direction of $D = 14.4^\circ$, $I = -72.1^\circ$ from five sites.

For the purpose of this work granodiorite and diabase dykes from the headland near Rasmussen Hut (sampling area about 100×100 m) and two subparallel mafic dykes on Rasmussen Island were sampled. Our results from gabbro and two subvertical mafic dykes of Rasmussen Island confirm the presence of one normal polarity component both in the gabbro ($D = 301.9^\circ$, $I = -81.4^\circ$) and in dykes ($D = 339.8^\circ$, $I = -82.3^\circ$; Fig. 3B). The results from granodiorites + dykes and pink granite near Rasmussen Hut area also show a N-polarity component with mean directions ($D = 21.9^\circ$, $I = -76.1^\circ$ and $D = 15.6^\circ$, $I = -71.2^\circ$) which is close to above-mentioned determination by Grunow (1993). The pink granite samples are characterized by more scattered directions within the site ($\alpha_{95} = 12.7$) than the gabbro.

Scott Mount area. A single N-polarity component of NRM was detected in Duseberg Buttress diorites ($D = 31.5^\circ$, $I = -67.2^\circ$). The gabbros from Girard Bay also have a single N-polarity component with direction $D = 53.4^\circ$, $I = -65.1^\circ$ which is slightly different than in other sites (see Table 2) and probably due to local tectonics (overlapping pyroclastic rocks have tilted layers with dips to NE and NW). The bedding correction here is unclear as we do not know whether the gabbros intruded after or before the deformation of the area. The basalt samples from the bottom of Scott Mount show the scatter directions, but a stable N-polarity component has been isolated from 7 samples with $D = 31.5^\circ$, $I = -75.6^\circ$ which is close to the direction of Duseberg Buttress diorites.

NEIGHBOURING ISLANDS

Petermann Island. The sampling area stretches about 800 m along the coastline in the NNW part. Two distinct components of NRM were determined in gabbro and quartz-diorite samples. The normal polarity component with $D = 6.7^\circ$, $I = -67.9^\circ$ corresponds to the blocking temperature interval of $200\text{--}400^\circ\text{C}$ (further intermediate-temperature component

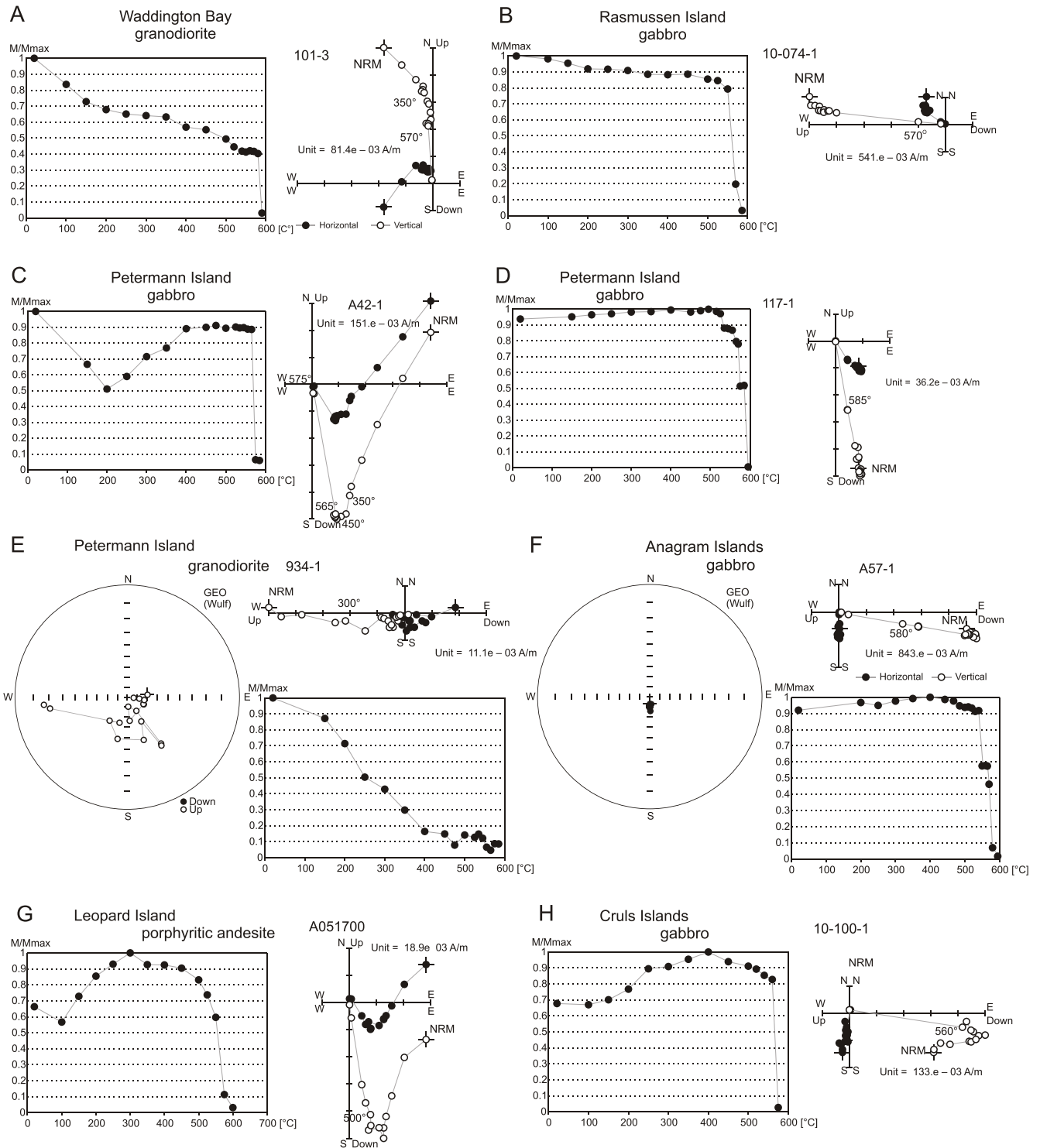


Fig. 3. Examples of typical thermal demagnetisation curves of specimens from the western coast of the Antarctic Peninsula (A–B) and adjacent islands (C–H)

The NRM intensity decay curve (left), orthogonal plot (right) and stereographic projections (for two samples) are shown. Open circles (solid circles) on the orthogonal diagrams are projections on the vertical (horizontal) planes at the indicated levels of thermal cleaning

Table 2

Site-mean palaeomagnetic directions and statistical parameters

No.	Site	Samples	Lithology	NRM [A/m]	Com- po- nent	n/N	D [°]	I [°]	K	α_{95} [°]	VGP Lat. °S	VGP Long. °E	Com- po- nent polar- ity
Cape Tuxen and Deliverance Point													
1	Cape Tuxen (64.11°W 65.27°S)	140–153 A23–A27	gabbro	$\frac{0.8-4.7}{2.5}$		15/19	2.8	-79.1	128	3.4	86.1	280.6	N
2	Deliverance Point (64.08°W 65.31°S)	84–94	granodiorite	$\frac{0.3-0.5}{0.4}$		13/13	28.5	-77.5	161	3.3	78.3	222.5	N
3	Waddington Bay (64.05°W 65.29°S)	96–101 105–106	granodiorite	$\frac{0.1-0.7}{0.4}$		8/8	13.2	-76.4	307	3.2	84.3	201.5	N
Moot Point (64.07°W, 65.2°S)													
4	Moot Point (mainland)	53–60 10/154–10/161 10/223–10/246	diorite	$\frac{0.07-1.0}{0.2}$		20/22	12.6	-69.6	53	4.5	76.6	150.2	N
5	Moot Point (island)	41–45 50–52	granodiorite	$\frac{0.05-0.6}{0.3}$		5/8	39.0	-63.8	30	14.3	61.1	182	N
Rasmussen Hut and Rasmussen Island (64.07°W, 65.25°S)													
6	Rasmussen Island	A28–A37	diabase (dyke)	$\frac{0.08-2.8}{1.06}$		10/10	339.8	-82.3	151	3.9	78.3	322.2	N
6'	Rasmussen Island	10/072–10/085	gabbro	$\frac{0.6-3.0}{1.6}$		7/13	301.9	-81.4	163	4.7	69.0	338.9	N
7	Rasmussen Hut	021–035 154–157	granodiorite + diabase (dyke)	$\frac{0.3-1.0}{0.6}$ $\frac{2.6-11.2}{5.4}$		18/20	21.9	-76.1	283	2.1	80.4	206.3	N
7'	Rasmussen Hut	10/117–10/126 10/148–10/154	pink granite	$\frac{0.005-0.1}{0.05}$		13/16	15.6	-71.2	12	12.7	76.0	158	N
Scott Mount area													
8	Duseberg Buttress (64.1°W 65.16°S)	131–137	diorite	$\frac{0.5-0.9}{0.7}$		6/7	31.5	-67.2	336	3.7	67.7	178.2	N
9	Mount Scott (64.08°W 65.16°S)	10/253–10/266	basalt	$\frac{0.006-0.5}{0.05}$		7/17	31.5	-75.6	334	3.2	76.1	210.8	N
10	Girard Bay (64.0°W, 65.13°S)	158–165	gabbro	$\frac{0.3-2.0}{1.1}$		8/8	53.4	-65.1	496	2.5	56.7	199.8	N
Petermann Island (64.15°W, 65.17°S)													
11	Petermann Island	107–120 A38–A45 938–942	gabbro + quartz- diorite	$\frac{0.2-6.0}{1.7}$ $\frac{0.02-0.07}{0.03}$	HTC	27/27	154.4	76.3	156	2.2	79.0	20.5	R
11'		107–120 A38–A45 941,942	gabbro		ITC	19/27	6.7	-67.9	22.8	7.2	75.3	132.8	N
11''		933–937 10/133–10/147	granodiorite		ITC	7/20	350.3	-73.6	15	16.1			N
Berthelot Islands (64.13°W, 65.33°S)													
12	Berthelot Islands	16–20 A58–A64	gabbro	$\frac{0.2-1.0}{0.5}$		12/12	359.9	-76.2	184.7	3.2	88.5	114.3	N
13		001–015	granodiorite	$\frac{0.06-0.3}{0.16}$		13/14	9.2	-78.4	55	5.6	85.7	242.4	N
Argentine Islands Archipelago (64.25°W, 65.25°S)													
14	The Barchans (64.32°W 65.23S)	38–40 835–856	granodiorite	$\frac{0.04-0.4}{0.17}$	HTC	22/24	151.1	81.8	102	3.1	76.9	332.1	R
14'					ITC	12/24	334.7	-81.4	34	7.6	78.2	332.7	N

Tab. 2 cont.

No.	Site	Samples	Lithology	NRM [A/m]	Component	n/N	D [°]	I [°]	K	α_{95} [°]	VGP Lat. °S	VGP Long. °E	Component polarity
15	Anagram Islands (64.32°W 65.2°S)	A51–A57 10/186–10/193 10/164–10/171	gabbro	<u>1.5–12.0</u> 3.4		22/24	176.3	78.0	195	2.2	87.6	333.1	R
16	Leopard, Black, Winter Islands	AO105–108, AO506–520, AO545–551	porphyritic andesites	<u>0.03–1.2</u> 0.1	HTC	16/25	186.5	79.4	55	5.0	85.1	267.8	R
16'					ITC	14/25	8.9	–66.1	13	11.7	72.5	135.6	N
Roca Islands and Cruls Islands (64.48°W, 65.19°S)													
17	Roca Islands (64.48°W 65.19°S)	61–72	granodiorite	<u>0.05–0.5</u> 0.26	HTC	8/10	180.0	83.7	91.5	5.8	77.6	295.5	R
17'					ITC	7/10	27.8	–72.5	6.2	26.4	75.0	170.8	N
18	Cruls Islands (64.53°W 65.18°S)	A46–A50	diabase (dyke)	<u>0.1–1.1</u> 0.4	HTC	5/5	358.1	62.0	7	30.6			R
18'					ITC	5/5	324.2	–75.7	16	19.6			N
19	Cruls Islands (64.54°W 65.19°S)	10/099–10/111	gabbro	<u>0.4–0.9</u> 0.6	HTC	12/14	167.3	77.0	28	8.3	84.7	18.3	R
19'					ITC	4/14	334.5	–80.1	10	31.8			N
20	Cruls Islands (64.54°W 65.19°S)	071–083	granodiorite	<u>0.01–0.2</u> 0.06		5/12	187.9	82.9	35	13.2	78.9	284.5	R
Port Lockroy (63.5°W, 64.83°S) Wiencke Island													
21	Port Lockroy	167–180	granodiorite	<u>0.1–8.0</u> 1.7		9/12	219.5	84.3	338	2.8	72.1	272.6	R

No – number of site in accordance with Figure 4; ITC – intermediate temperature component; HTC – high temperature component; NRM – diapason (underlined) and mean natural remanent magnetisation; n/N – number of samples used for site mean calculation/total number of samples; D – declination, I – inclination; α_{95} – radius of 95% confidence cone around mean direction; K – estimate of precision parameter; VGP Lat., Long. – latitude and longitude of palaeopoles; polarity: N – normal, R – reversed

ITC), but the high temperature interval 450–580°C shows a reverse polarity component (further high temperature component HTC) with mean direction $D = 154.4^\circ$, $I = 76.3$ (Fig. 3C). This high temperature reverse polarity component is clearly distinguished in all samples investigated between 450–600°C, going through the origin in the diagrams (Fig. 3D). Three quartz-diorite samples showed the same behavior of the demagnetisation curve with a HTC and they are included in the statistics (Table 2).

The granodiorite samples from the central to the eastern part of the island are characterized by unstable remanence and a scatter of directions during the heating. Only from a few samples can we isolate the ITC N-polarity component decaying between 200–400°C (Fig. 3E), whereas the HTC could not be distinguished because of a large spread of directions between neighboring steps of demagnetisation. This HTC R-polarity component was isolated in the four granodiorite samples from the western part of Hovgaard Island (one km north from Petermann Island) with mean direction $D = 255.4^\circ$, $I = 76.1^\circ$ and $\alpha_{95} = 14.5$ (it is not included in Table 2).

Berthelot Islands. The sampling area covers 50×300 m on the NE part of the largest island. Single N-polarity components were isolated in both gabbros and granodiorites with mean directions $D = 359.9^\circ$, $I = -76.2^\circ$ and $D = 9.2^\circ$, $I = -78.4^\circ$, respectively (Table 2), are close to the mean palaeodirection

($D = 358^\circ$, $I = -72^\circ$) obtained from 8 gabbro samples by Blundell (1962).

Argentine Islands Archipelago. The samples were taken on the three largest Barchans Islands (granodiorites), on the two largest islands of the Anagram Islands Archipelago (gabbros) and on the three islands (Leopard, Black, Winter) in the southern part of the archipelago.

Palaeomagnetic data from the Barchans Islands, except for a viscous component, revealed the two-component NRM with the shape of demagnetisation curves very similar to those from Petermann Island. The normal polarity ITC with blocking temperatures of between 200–400–500°C has $D = 334.7^\circ$ and $I = -81.4^\circ$. The HTC is reversed with $D = 151.1^\circ$, $I = 81.8^\circ$. This direction is close to values found by Blundell (1962) from 12 quartz-diorite samples from the same area ($D = 144^\circ$, $I = 82^\circ$).

The gabbros from the Anagram Islands (Nob Island and an unnamed middle island) have a single stable component of NRM (Fig. 3F) of R-polarity with mean direction $D = 176.3^\circ$ and $I = 78.0^\circ$, which is close to the HTC determined in the Barchans granodiorites. Some samples from Nob Island are characterized by high values of NRM (about 10 Am^{-1}) which are associated with a high content of magnetite (up to 30%) in these rocks (Bakmutov *et al.*, 2009).

The islands on the south of archipelago are composed mainly of porphyritic andesites. We combine the data from

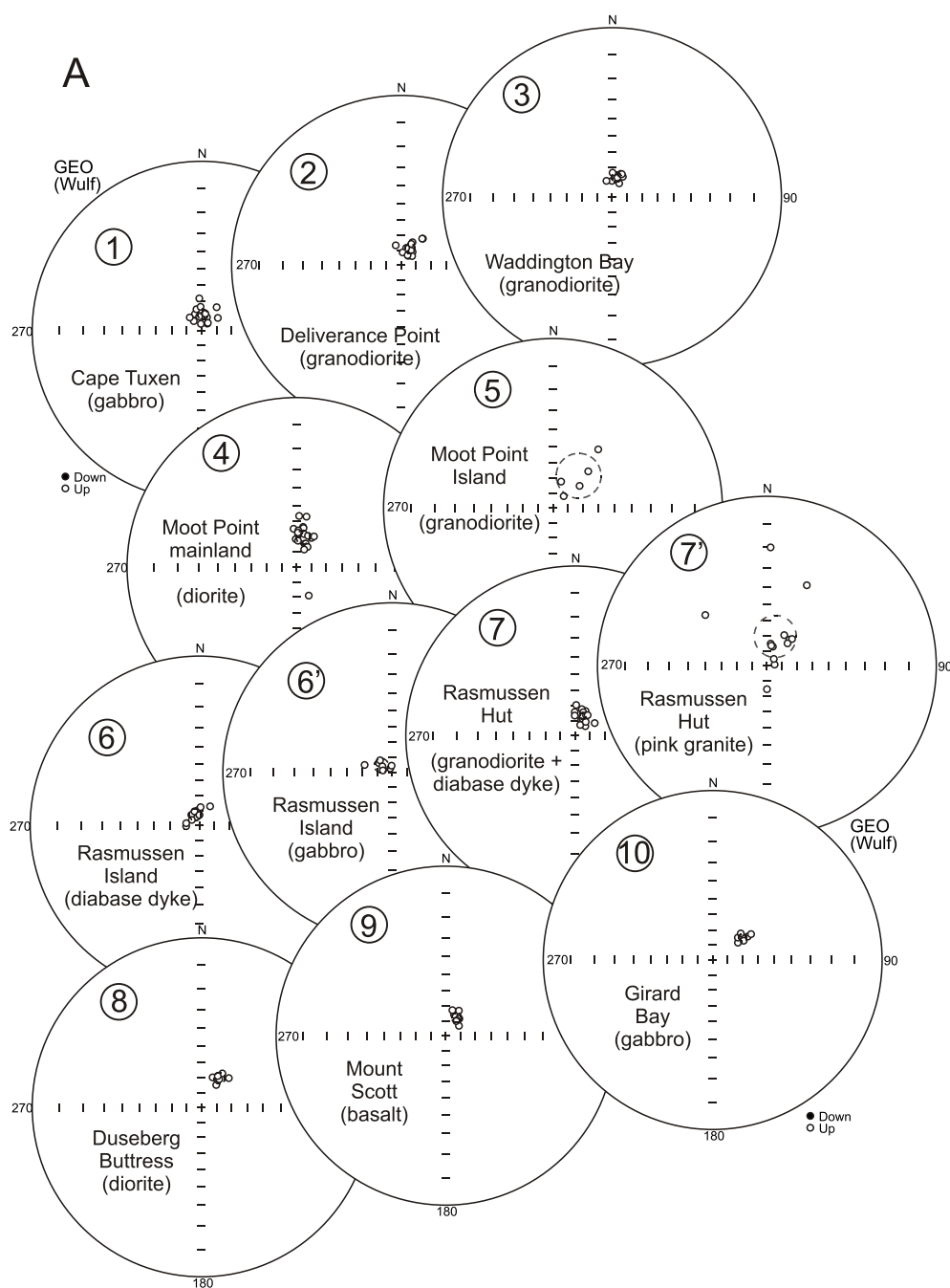


Fig. 4A – stereographic projections of line-fit palaeomagnetic directions of specimens of HTC-components

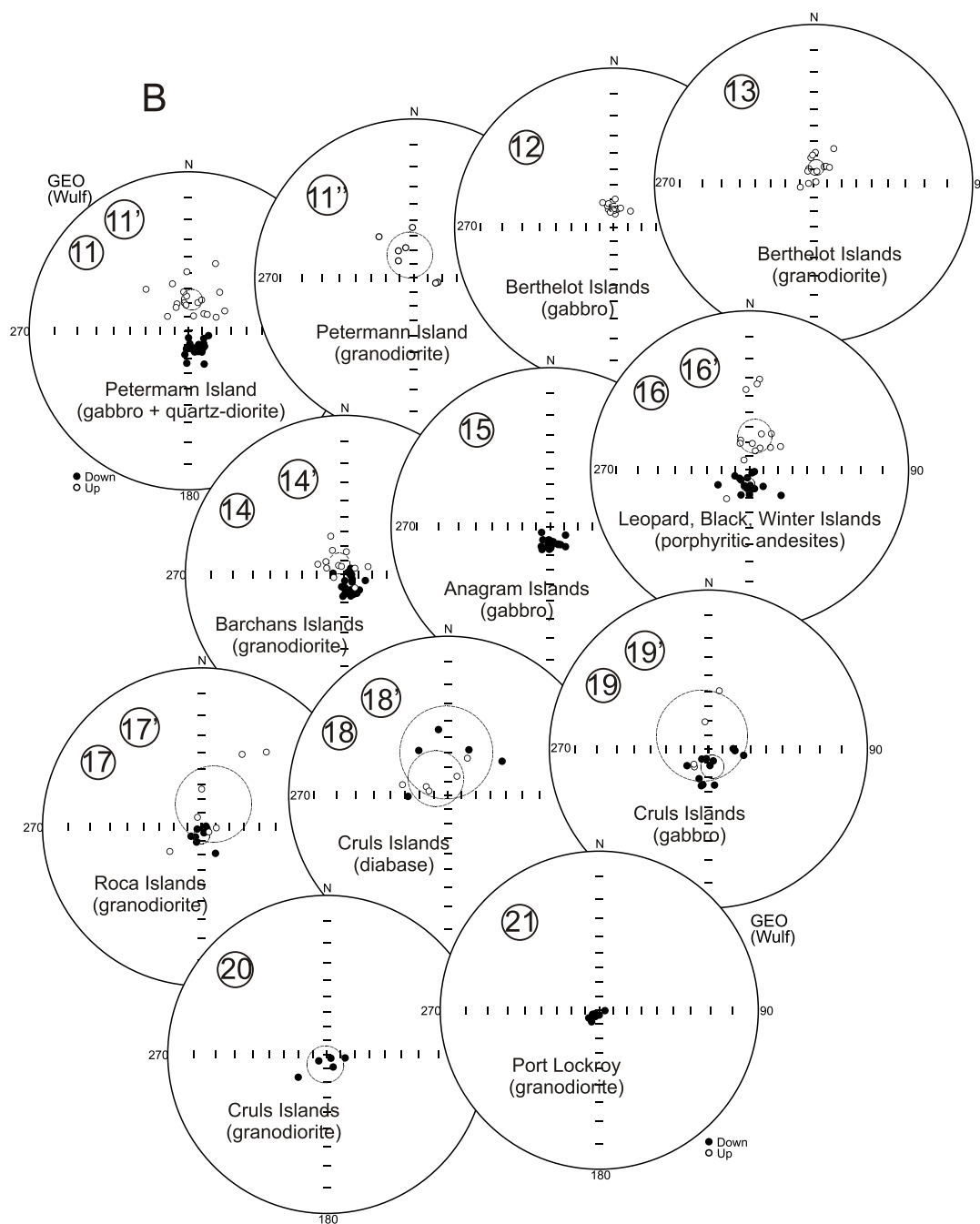
The numbers of sites are corresponds to N in Table 2; open (close) symbols denote upward (downward) pointing inclinations;

Leopard, Black and Winter Islands to one site because there are not enough samples for statistics from each island and we have no direct age determination from these rocks. Taking into account the above-mentioned ages of the Argentine Islands the porphyritic andesites may be referred to the Paleocene. The palaeomagnetic results indicate the ITC N-polarity and HTC R-polarity components with directions of $D = 8.9^\circ$, $I = -66.1^\circ$ and $D = 186.5^\circ$, $I = 79.4^\circ$ respectively (Fig. 3G).

Roca and Cruls Islands. A few km to the NW of the Argentine Islands Archipelago, two groups of islands named Roca and Cruls were selected for palaeomagnetic sampling.

The rocks are represented by gabbros and granodiorites with comagmatic dykes. There are no direct age determinations here, but the age considering the geological background of the region should be Paleocene.

The ITC N-polarity and HTC R-polarity components have been isolated in granodiorite samples from the Roca Islands and gabbro and diabase (dyke) samples from Cruls Islands (Table 2). Only a few samples from the granodiorite of the Cruls Islands are characterized by stable remanence (Fig. 3H). The samples from a diabase dyke and a large number of granodiorite samples from Cruls Islands are characterized by scattered palaeomagnetic di-



from the igneous rocks studied from the Antarctic Peninsula coast; B – HTC- and ITC-components from neighbouring islands

dashed circles are the radius of the 95% confidence cone of mean directions

rections during stepwise demagnetisation that do not allow inclusion of this data into the statistics.

Wiencke Island (Port Lockroy). The sampling was performed along the sea coast of the promontory opposite the old British base Port Lockroy. All samples show only single R-polarity components with a mean direction of $D = 219.5^\circ$, $I = 84.3^\circ$.

DISCUSSION

Site coordinates and site-mean directions, with the associated statistical parameters for all rocks investigated are shown in Figure 4A and B and are listed in Table 2.

The results of thermal demagnetisation of gabbroid samples showed pronounced decay of the remanence between about 540°C and 590°C and a single ChRM component of normal (Fig. 3B) or reversed (Fig. 3D, F) polarity. Most of the gabbroid sites display behaviour of demagnetisation curves in a similar fashion, like those of Figure 3D and F. Some samples have small or no overprint magnetisations that may have been introduced by recent growth of a viscous remanence (removed by $150\text{--}200^\circ\text{C}$ heating; Fig. 3C). Other samples shown nearly univectorial decay but two phases on the demagnetisation curves, one set unblocking around $350\text{--}500^\circ\text{C}$ and an other unblocking in the interval $540\text{--}590^\circ\text{C}$ (Fig. 3H).

The granodiorites usually have relatively low values of magnetic susceptibility and NRM intensity and are characterized by more scattered directions in comparison to the gabbros (compare α_{95} in Table 2). The ChRM are characterized by both normal and reversed polarities. Demagnetisation curves and orthogonal plots show mainly a single component of remanence (HTC), but some samples reveal the presence of an ITC with the same directions as the HTC (Fig. 3A). From some samples the HTC could not be isolated (Fig. 3E); in some samples we could not distinguish any directions of remanence because of a wide scatter between neighbouring steps of demagnetisation. The granodiorites site means and statistic parameters (Table 2 and Fig. 4) show directions similar to those for the gabbros, but with a larger scatter of data within the site.

Summarizing this short review of magnetic mineralogy we underline that the dominant mineral in the rocks studied is the magnetite and the main carrier of the NRM is the small SD-PSD fraction with an unblocking temperature of 540–590°C. There is no evidence for remagnetisation of these rocks. The magnetisation is mainly primary. The same palaeomagnetic directions have been isolated from different types of rocks (gabbros, diorites, granodiorites, porphyritic andesites and diabases).

Most of our palaeomagnetic results correspond to two main age groups: one yielding ages 84–117 Ma and the other of about 60 ± 10 Ma (Table 1). The rocks sampled along the AP coast (Fig. 5A) belong to the Cretaceous Normal Superchron (CNS). Here all the samples are characterized by a single component of magnetisation clearly observed after removal of a small soft component which is likely of viscous origin. The

mean palaeodirections (Table 2 and Fig. 4A) lie close to the data reported previously (Blundell, 1962; Grunow, 1993). Thus, it is likely that the primary NRM of these rocks corresponds to the same time interval between 117–84 Ma.

For the sites collected on the islands, radiometric dating provided ages of 50–73 Ma (an exception is Petermann Island), which are outside of the CNS. Their ChRM vectors are of both N-polarity (Berthelot Islands, 73 Ma) and R-polarity (other islands) with mean direction of $D = 176.4^\circ$; $I = 80.1^\circ$ (Fig. 5B).

Combining the ages and polarities we can conclude that they agree with the geomagnetic polarity time scale (GPTS) (Gradstein *et al.*, 2004) with the exception of the Petermann Island results. Despite two radiometric ages (93 Ma by Rb-Sr and 96 Ma by U-Pb), the ChRM of the gabbro samples are characterized by a single component HTC of R-polarity (example on Fig. 3D) while some samples also have an ITC N-polarity component (example on Fig. 3E). The directions of these components are coincident with the directions of HTC and ITC components from other sites. This fact may be explained via different hypotheses. We are not excluding: (a) the self-reversal phenomenon of the NRM in these samples; (b) a short event of reversed polarity inside the CNS (*cf.* Gradstein *et al.*, 2004); (c) complete re-magnetisation of the NRM at some time younger than the CNS (due to a later granodiorite intrusion); (d) the U/Pb zircon crystallization ages obtained for magmatic rocks in the area studied that precedes the ChRM by millions of years.

We do not have any data which confirm scenario (a). With scenario (b) we suggest that the NRM is indeed the primary TRM but that the rocks were generated during a short period of reverse polarity which is missed in the contemporary geomag-

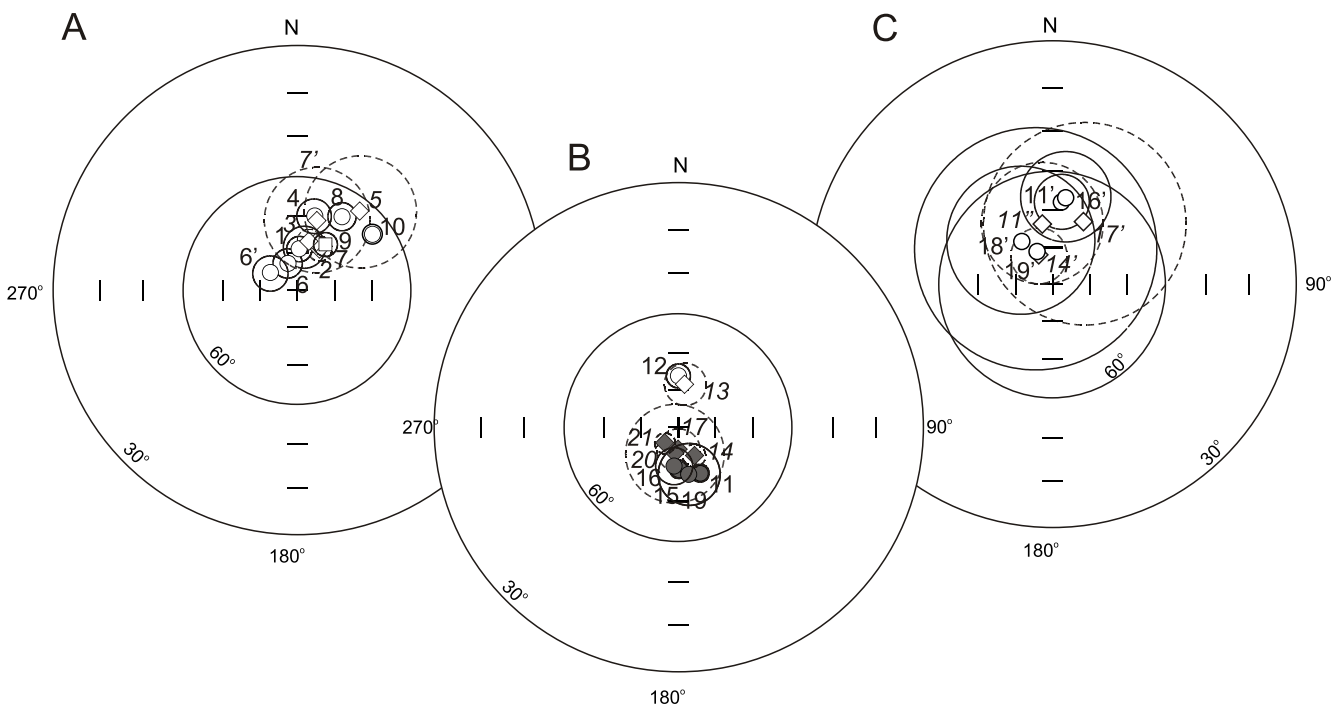


Fig. 5. Site mean directions with α_{95} obtained from gabbros (circles), granitoids (rhombs) and basalts (squares)

A – directions of high temperature components of NRM for sites of Late Cretaceous age; B – the same for the Paleocene sites; C – directions of the low temperature ITC-component; the numbers near the symbols indicate the site identification number as shown in Table 2; granitoids numbers are given in italic, α_{95} for gabbros (granitoids) are given by continuous (dashed) circles; open (solid) symbols correspond to projection onto the upper (lower) hemisphere

netic polarity time scales. For this reason we will sustain this data in our future analysis though underline once more that the results may be subject to doubt. Scenario (c) seems unlikely because there is no evidence of alteration in gabbros. As regards scenario (d), the recent results from the Petermann Island granitoids (Guenther *et al.*, 2010) indicate that the low-temperature thermochronology data is at least 50 million years younger than the 93–96 Ma ages reported above. The zircon (U-Th)/He (zircon He) with a closure temperature of about 170–200°C and zircon fission track (zircon FT) data with a closure temperature of about 220–260°C show ages of 42.8 ± 0.9 and 35.6 ± 4.2 Ma respectively and long-term cooling phase with moderate rates ($\sim 3^\circ\text{C}/\text{Ma}$) from 40 to 10 Ma (Guenther *et al.*, 2010). Nevertheless, we retain the results in the Table 3 considering that the age of these rocks is younger than the CNS.

The mean palaeomagnetic direction from sites along the Antarctic Peninsula coastline (N = 12, D = 22.9°, I = -75.0°, Table 3, Fig. 5A) have a slightly different declination in comparison with those reported by Grunow (1993) for the mean direction of 6 sites (Cape Tuxen and Deliverance Point, D = 4.7°, I = -75.2°) and by Poblete *et al.* (2011), obtained for igneous rocks of the same ages from the Gerlache Strait area (D = 3.3°, I = -74.9°).

The mean palaeomagnetic pole calculated for these sites (79.3°S, 197.9°E) has been compared with previous data from this area (Grunow, 1993; Poblete *et al.*, 2011) and with a synthetic apparent polar wander path (APWP) for East Antarctica (Fig. 6A; Besse and Courtillot, 2002; Torsvik *et al.*, 2008). These two updated curves were derived from a global compilation of the palaeomagnetic poles from different plates with different sea-floor spreading histories. There are slight differences between both APWPs for the last 140 Ma, in particular from 90 to 70 Ma – counterclockwise loop (Besse and Courtillot, 2002) contrasting with direct drift (Torsvik *et al.*, 2008). Unfortunately, there is no palaeomagnetic data available directly for East Antarctica for the Late Cretaceous–Paleocene and the shape of this part of curve is not clear.

Our new pole for 117–84 Ma is close to the reference for the APWP 110 Ma time interval (Besse and Courtillot, 2002; Torsvik *et al.*, 2008; Fig. 6A), but departs slightly from the APWP of 112, 100 and 90 Ma reported for the Antarctic Peninsula by Poblete *et al.* (2011; Fig. 6B).

Grunow (1993) save palaeomagnetic results from intrusive rocks at Cape Tuxen, Moot Point and Rasmussen Island which were dated respectively at 85, 107 and 117 Ma. Our high-precision palaeomagnetic data are from the same points. We combined the results from these three points (mean directions from table 2 in Grunow, 1993) with our new data from the same points to provide mean poles for 117–107 Ma (assigned age 112 Ma on the Fig. 6B) and 85 Ma (Fig. 6B and Table 3). These well-dated two palaeomagnetic poles (81.5°S, 183.2°E and 85.6°S, 207.4°E respectively) are close to each other (overlapping at α_{95} confidence levels). If we compare these poles with the APWP for East Antarctica given by Torsvik *et al.* (2008), exactly the same pole position of the reference APWP between 110–100 Ma (lag in age between our data and reference APWP is about 7 Ma) and of 100 Ma (lag is about 15 Ma) can be recognized. This lag can be attributed to the difference between the closure temperature of the U-Pb system in zircon (about 900°C) and the blocking temperatures range of the HTC component in the interval 540–590°C.

The mean palaeomagnetic directions of the HTC- and ITC-components from the islands (Fig. 5B, C) and mean positions of palaeopoles are given in Table 3. Taking into account a wide spread of geochronological ages of Paleocene sites from the islands we assigned a mean age of 60 Ma for the ChRM HTC-component. This palaeomagnetic pole (Fig. 6B) fits well to the APWP given by Torsvik *et al.* (2008) in the time interval 50–30 Ma, but departs slightly from the Paleocene poles reported by Nawrocki *et al.* (2010) and from the combined palaeomagnetic pole for 60 Ma reported by Poblete *et al.* (2011) for the South Shetland Islands. This departure has a common direction and magnitude of about 12–16°.

Most of the Cenozoic palaeomagnetic poles from West Antarctica were isolated from the islands surrounding the AP.

Table 3

Mean palaeodirections and palaeopoles

Time interval [Ma]	Location	D [°]	I [°]	K	α_{95} [°]	N	Pole Lat. °S	Pole Long. °E	pole dp	pole dm
Results with an attribute to Cretaceous age (this paper)										
84–117	Antarctic Peninsula (Table 2, N1–10)	22.9	-75.0	80	4.9	12	79.3	197.9	8.1	8.9
Results with an attribute to Cretaceous age, this paper, combined with data from Grunow (1993).										
107–117 (112)	(Table 2, N4–7 and Grunow, 1993)	16.3	-74.4	89	5.5	9	81.5	183.2	9.0	10.0
85	(Table 2, N1–3 and Grunow, 1993)	10.5	-76.8	665	3.0	5	85.6	207.4	5.5	5.7
Results with an attribute to Paleocene age (this paper)										
50–75	Islands (Table 2, N11–21, HTC-component)	176.4	80.1	351	2.6	10	83.4	307.6	4.7	5.0
50–75	Islands (Table 2, N112–1, ITC-component)	357.4	-74.9	96	6.2	7	86.2	263.3	10.3	11.3

Overall mean directions of the gabbros and granodiorite collections and palaeopoles with the semi-major and semi-minor axes of the oval of 95% confidence (dm, dp); other explanations as in Table 2

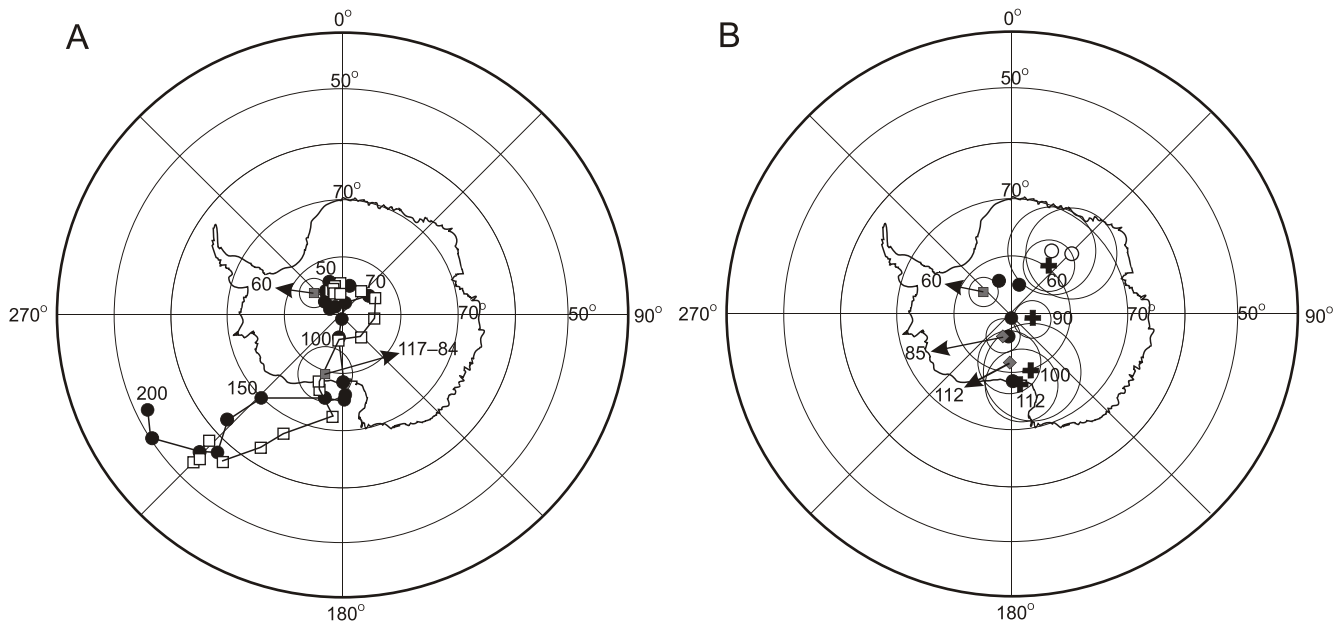


Fig. 6A – apparent polar wandering paths for East Antarctica from Torsvik *et al.* (2008; black dots) and Besse and Courtillot (2002; white squares), and our palaeopoles for 117–84 Ma and 75–50 Ma (gray squares with α_{95} ovals); **B** – virtual geomagnetic poles obtained in this study for 112, 85 Ma (gray rhombs) and 60 Ma (gray squares)

Black cross (with ages) – palaeopoles obtained at 112, 110 and 90 Ma for the Antarctic Peninsula and 60 Ma for South Shetland Islands by Poblete *et al.* (2011); open circles – palaeopoles obtained for Point Thomas Formation and Znosko Glacier Formation for South Shetland Island (about 50 Ma) by Nawrocki *et al.* (2010); all data are given with α_{95} ovals; the reference poles at 110, 100, 90, 60 and 50 Ma (the same as on the Fig. 6A) are shown as black circles

The South Shetland Islands palaeomagnetic data provided the best quality Paleocene poles in the AP published earlier (Dalziel *et al.*, 1973; Watts *et al.*, 1984; Grunow, 1993; Nawrocki *et al.*, 2010; Poblete *et al.*, 2011). This data shows a similar counterclockwise rotation with respect to the reference APWP to that suggested by Besse and Courtillot (2002) and Torsvik *et al.* (2008). In accordance to Nawrocki *et al.* (2010), the observed departure of palaeomagnetic poles reflects discrete anticlockwise tectonic rotations of particular tectonic blocks of King George Island that took place after the early Eocene (*ca.* 50 Ma).

Both of the Late Cretaceous and Paleocene groups of our palaeomagnetic poles confirm that the AP has been at nearly at the same high palaeolatitude during the last 100 Ma as were reported earlier (Grunow, 1993; Nawrocki *et al.*, 2010; Poblete *et al.*, 2011). For the Paleocene poles the difference in declination between the northern block (King George and neighbour islands) and our sites is apparent. Our Paleocene palaeopol latitude is about 4–8° upper than the coeval latitudes calculated from the South Shetland Islands (Fig. 6B). Therefore we cannot exclude the palaeomagnetically detectable rotation of the South Shetland Islands and in particular of King George Island as interpreted by Nawrocki *et al.* (2010).

The palaeomagnetic pole calculated for the ITC-component for islands (86.2°S, 263.3°E; Table 3) is close to the APWP of Torsvik *et al.* (2008) for 10 Ma to the present day and could be interpreted as a recent viscous component.

The observed inclination at 112, 85 and 60 Ma are within 2° of the expected inclination determined from the synthetic APWP of Torsvik *et al.* (2008), Besse and Courtillot (2002)

and from our data confirm the lack of latitudinal displacement of the AP with respect to East Antarctica.

CONCLUSIONS

1. New palaeomagnetic data from the Late Cretaceous-Paleocene plutonic rocks of the AP batholith have been obtained. The magnetisation of these rocks is mainly primary. The same palaeomagnetic directions have been isolated from volcanic and intrusive rocks which have different chemical compositions (gabbros, diorites and quartz-diorites, tonalites, granites, granodiorites, porphyritic andesites, basalts). Our data agree with previous palaeomagnetic determinations established in this area.

2. The rocks along the coastline of the western part of the AP coast can be correlated with the Cretaceous Normal Superchron while all the rocks from the islands with reversed polarity reflect the Paleocene geomagnetic field.

3. Well-dated palaeomagnetic poles for the time interval 117–84 Ma (subdivided into 112 Ma and 84 Ma) fit well to the synthetic APWP for East Antarctica (Torsvik *et al.*, 2008) being located between 110–100 Ma and close to the APWP of 112, 100 and 90 Ma reported for the Antarctic Peninsula by Poblete *et al.* (2011). This confirms that the AP did not undergo latitudinal displacement for the last 100 Ma.

4. A common characteristic direction was obtained from Paleocene igneous rocks, which suggests a common origin of their magnetisation. The palaeomagnetic pole obtained for 60 Ma fits well to the APWP of Torsvik *et al.* (2008), but

slightly departs from the group of palaeomagnetic poles of the AP, which have been obtained mainly from the South Shetland Block. This implies that the South Shetland Islands had their own tectonic evolution and probably anticlockwise rotation caused by local tectonics during the Paleocene.

5. The interpretation of age and the magnetic polarity of rocks from Petermann Island is still open. The simplest explanation – an episode of reverse polarity in CNS – is not sufficient. This phenomenon requires additional palaeomagnetic and age determinations.

Acknowledgement. This study was partly supported by a grant of the Ukrainian Fundamental Research State Fund (F40.6/030). We gratefully acknowledge the National Ukrainian Antarctic Center for support of our research in West Antarctica. Special thanks to the Ukrainian wintering teams on Akademik Vernadsky base which provided the logistic support for field work during the season's expeditions. We are grateful to J. Nawrocki and M. K. Działko-Hofmokl for careful reviews, which helped improve the manuscript, and J. Zalasiewicz for language corrections.

REFERENCES

- BAKHMUTOV V. G., ARTEMNKO G. V., GLADKOCHUB D. P. and SAMBORSKAJA I. A. (2009) – Geochemistry and ore-bearing mafic intrusion of Antarctic Peninsula (in Russian). XLII Tectonic Meeting, Moscow. *GEOS*, **1**: 49–52.
- BARKER P. F. (2001) – Scotia Sea regional tectonic evolution: implications for mantle flow and palaeocirculation. *Earth Sc. Rev.*, **55**: 1–39.
- BESSE J. and COURTILOT V. (2002) – Apparent and true polar wander and the geometry of the geomagnetic field over the last 200 Myr. *J. Geoph. Res.*, **107** (B11): 2300, doi:10.1029/2000JB000050
- BLUNDELL D. J. (1962) – Paleomagnetic investigations in the Falkland Islands Dependencies. *British Antarctic Surv. Rep.*, **39**.
- CHADIMA M. and HROUDA F. (2006) – Remasoft 3.0 – a user-friendly palaeomagnetic data browser and analyzer. *Travaux Géophysiques*, **27**: Abstracts of the 10th “Castle Meeting”. New Trends in Geomagnetism. Castle of Valtice, 3–8 September 2006: 20–21.
- CUNNINGHAM W. D., DALZIEL I. W. D., LEE T. Y. and LAWVER L. A. (1995) – Southernmost South America–Antarctic Peninsula relative plate motions since 84Ma: implications for the tectonic evolution of the Scotia Arc region. *J. Geoph. Res.*, **100**: 8257–8266.
- CURTIS R. (1966) – The petrology of the Graham Coast, Graham Land. *British Antarctic Surv. Rep.*, **50**.
- DALZIEL I. W. D. and ELLIOT D. H. (1982) – West Antarctica: problem child of Gondwanaland. *Tectonics*, **1**: 3–19.
- DALZIEL I. W. D. and LAWVER L. A. (2001) – The lithospheric setting of the West Antarctic Ice Sheet. In: *The West Antarctic Ice Sheet; Behavior and Environment* (eds. R. B. Alley and R. A. Bindshadler): 29–44. Antarctic Research Series. American Geophysical Union, Washington, D.C.
- DALZIEL I. W. D., LOWRIE W., KLINGFIELD R. and OPDYKE N. D. (1973) – Paleomagnetic data from the southernmost Andes and the Antarctic. In: *Implications of Continental Drift to the Earth Sciences* (eds. D. H. Tarling and S. K. Runcorn). Acad., New York., **1**: 87–101.
- DAY R., FULLER M. and SCHMIDT V. A. (1997) – Hysteresis properties of titanomagnetites: grain-size and compositional dependence. *Phys. Earth Planet. Internat.*, **13**: 260–267.
- ELLIOT D. H. (1964) – The petrology of the Argentine Islands. *British Antarctic Surv. Rep.*, **41**.
- FERRACCIOLI F., JONES P. C., VAUGHAN A. P. and LEAT P. T. (2006) – New aerogeophysical view of the Antarctic Peninsula: more pieces, less puzzle. *Geoph. Res. Lett.*, **33** (5), L05310, doi:10.1029/2005GL024636
- FLEMING E. A. and THOMSON J. W. (1979) – Northern Graham Land and South Shetland Islands. In: *British Antarctic Territory Geological Map*, 1:500 000 scale. British Antarctic Survey, Cambridge.
- GLADKOCHUB D., BAKHMUTOV V., VODOVOZOV V. and VASCHENKO V. (2009) – West Antarctica Andean complex: age, compound, geodynamic position (in Russian). In: *Geology of the Earth's Polar Regions*. XLII Tectonic Meeting, Moscow. *GEOS*, **1**: 132–134.
- GRIKUROV G. E. (1973) – Geology of the Antarctic Peninsula (in Russian). Nauka, Moscow.
- GHIDELLA M. E., YÁ EZ G. and LABRECQUE J. L. (2002) – Revised tectonic implications for the magnetic anomalies of the western Weddell Sea. *Tectonophysics*, **347**: 65–86.
- GRADSTEIN F. M., OGG J. G. and SMITH A. G. (2004) – A geologic time scale 2004. Cambridge University Press.
- GRUNOW A. M. (1993) – New paleomagnetic data from Antarctic Peninsula and their tectonic implication. *J. Geoph. Res. Solid Earth*, **98**: 13815–13833.
- GUENTHNER W. R., BARBEAU jr. D. L., REINERS P. W. and THOMSON S. N. (2010) – Slab window migration and terrane accretion preserved by low-temperature thermochronology of a magmatic arc, northern Antarctic Peninsula. *Geochem. Geoph. Geosyst.*, **11**, Q03001, doi: 10.1029/2009GC002765
- HOOVER P. R. (1962) – The petrology of Anvers Island and adjacent islands. *British Antarctic Surv. Rep.*, **34**.
- KELLOGG K. (1980) – Paleomagnetic evidence for oroclinal bending of the southern Antarctic Peninsula. *Geol. Soc. Am. Bull.*, **91**: 414–420.
- KELLOGG K. and REYNOLDS R. L. (1978) – Paleomagnetic results from the Lassiter Coast, Antarctica, and a test for oroclinal bending of the Antarctic Peninsula. *J. Geoph. Res. Solid Earth*, **83**: 2293–2299.
- KIRSCHVINK J. L. (1980) – The least squares line and plane and the analysis of palaeomagnetic data. *Geoph. J. R. Astron. Soc.*, **62**: 699–718.
- LARTER R. D. and BARKER P. F. (1991) – Effects of ridge crest-trench interaction on Antarctic-Phoenix spreading: forces on a young subducting plate. *J. Geoph. Res.*, **96** (B12): 19583–19607, doi: 10.1029/91JB02053
- LARTER R. D., CUNNINGHAM A. P., BARKER P. F., GOHL K. and NITSCHKE F. P. (2002) – Tectonic evolution of the Pacific margin of Antarctica 1. Late Cretaceous tectonic reconstructions. *J. Geoph. Res.*, **107** (B12), 2345, doi: 10.1029/2000JB000052
- LEAT P. T., SCARROW J. H. and MILLAR I. L. (1995) – On the Antarctic Peninsula batholith. *Geol. Mag.*, **132** (4): 399–412.
- LONGSHAW S. K. and GRIFFITHS D. H. (1983) – A paleomagnetic study of Jurassic rocks from the Antarctic Peninsula and its implications. *J. Geol. Soc.*, **140**: 945–954.
- NAWROCKI J., PA CZYK M. and WILLIAMS I. S. (2010) – Isotopic ages and palaeomagnetism of selected magmatic rocks from King George Island (Antarctic Peninsula). *J. Geol. Soc., London*, **167**: 1063–1079, doi: 10.1144/0016-76492009-177
- PANKHURST R. J. (1982) – Rb–Sr chronology of Graham Land, Antarctica. *J. Geol. Soc., London*, **139**: 701–712.
- PANKHURST R. J. (1983) – Rb–Sr constraints on the ages of basement rocks of the Antarctic Peninsula. In: *Antarctic Earth Science* (eds. R. L. Oliver, P. R. James and J. B. Jago): 367–371. Australian Academy of Science, Canberra and Cambridge University Press, Cambridge.
- PARÉS J. M. and DINARÈS-TURELL J. (1999) – Datos paleomagnéticos del sustrato rocoso de la isla de Livingston (Península Antártica):

- implicaciones tectónicas en la evolución neógena. *Acta Geol. Hisp.*, **34**: 339–351.
- POBLETE F., ARRIAGADA C., ROPERCH P., ASTUDILLO N., HERVÉ F., KRAUS S. and LE ROUX J. P. (2011) – Paleomagnetism and tectonics of the South Shetland Islands and the northern Antarctic Peninsula. *Earth and Planet. Sc. Lett.*, **302**: 299–313.
- REX D. C. (1976) – Geochronology in relation to the stratigraphy of the Antarctic Peninsula. *British Antarctic Surv. Bull.*, **43**: 49–58.
- RILEY T. R., LEAT P. T., PANKHURST R. J. and HARRIS C. (2001) – Origins of large volume rhyolitic volcanism in the Antarctic Peninsula and Patagonia by crustal melting. *J. Petrol.*, **42** (6): 1043–1065.
- SHCHERBAKOVA V. V., BAKHMUTOV V. G., SHCHERBAKOV V. P., ZHIDKOV G. V., SHPYRA V. V., SMIRNOVA Z. I. and SERGIENKO Y. S. (2009) – Palaeointensity and palaeodirection of the geomagnetic field during Cretaceous Superchron and Palaeocene from the Western Antarctica rocks (in Russian). *Ukrainian Antarctic J.*, **8**: 94–112.
- TANGEMAN J. A., MUKASAS B. and GRUNOW A. M. (1996) – Zircon U-Pb geochronology of plutonic rocks from the Antarctic Peninsula: Confirmation of the presence of unexposed Paleozoic crust. *Tectonics*, **15** (6): 1309–1324.
- THOMPSON M. R. A. and PANKHURST R. J. (1983) – Age of Post-Gondwanian calc-alkaline volcanism in the Antarctic Peninsula region. In: *Antarctic Earth Science* (eds. R. L. Oliver, P. R. James and J. B. Jago): 328–333. Australian Academy of Science, Canberra and Cambridge University Press, Cambridge.
- TORSVIK T. H., GAINA C. and REDFIELD T. F. (2008) – Antarctica and global paleogeography: from Rodinia, through Gondwanaland and Pangea, to the birth of the Southern Ocean and the opening of gateways. In: *Antarctica: A Keystone in a Changing World* (eds. A. K. Cooper, P. J. Barrett, H. Stagg, B. Storey, E. Stump, W. Wise and 10th ISEAS editorial team): 125–140. Proc. of the 10th International Symposium on Antarctic Earth Sciences. National Academies Press, Washington DC.
- VALENCIO D. A., MENDIA J. E. and VILAS J. F. (1979) — Paleomagnetism and K-Ar of Mesozoic and Cenozoic igneous rocks from Antarctica. *Earth Planet. Sc. Lett.*, **45**: 61–68.
- VAUGHAN A. P. M., PANKHURST R. J. and FANNING C. M. (2002) – A Mid-Cretaceous age for the Palmer Land event, Antarctic Peninsula: implications for terrane accretion timing and Gondwana palaeolatitudes. *J. Geol. Soc.*, **159** (2): 113–116.
- VAUGHAN A. P. M. and STOREY B. C. (2000) – The Eastern Palmer Land shear zone: a new terrane accretion model for the Mesozoic development of the Antarctic Peninsula. *J. Geol. Soc. London*, **157** (6): 1243–1256.
- WATTS D. R., WATTS G. G. and BRAMALL A. M. (1984) – Cretaceous and Early Tertiary paleomagnetic results from the Antarctic Peninsula. *Tectonics*, **3**: 336–346.
- WEAVER S. D., SAUNDERS A. D. and TARNEY J. (1982) – Mesozoic-Cenozoic volcanism in the South Shetland Islands and the Antarctic Peninsula: geochemical nature and plate tectonic significance. In: *Antarctic Geoscience* (ed. C. Craddock): 263–273. University of Wisconsin Press, Madison.
- WILLAN R. C. and KELLEY S. P. (1999) – Mafic dyke swarms in the South Shetland Islands volcanic arc: unravelling multiphasic magmatism related to subduction and continental rifting. *J. Geoph. Res.*, **104** (B10): 23051–23068.
- YEGOROVA T., BAKHMUTOV V., JANIK T. and GRAG M. (2011) – Join geophysical and petrological models for the lithosphere structure of the Antarctic Peninsula continental margin. *Geoph. J. Internat.*, **184**: 90–110, doi: 111/j.1365-246X.2010.04867.x